COBEM 2023 27TH INTERNATIONAL CONGRESS OF MECHANICAL ENGENEERING

ABCM Brazilian Society of Mechanical Sciences and Engineering
27th ABCM International Congress of Mechanical Engineering
December 04-08, 2023, Florianópolis-SC, Brazil

COB-2023-2357
NUMERICAL INVESTIGATION OF THE AERODYNAMICS AND AEROACOUSTICS EFFECTS OF A ZIGZAG TRIPPING ON AN AERONAUTICAL PROPELLER

Gabriel Caldeira Vicente
Mateus Grassano Lattari
Júlio Apolinário Cordioli
César José Deschamps
Federal University of Santa Catarina, Department of Mechanical Engineering, Florianópolis - SC, Postal Code 88040-900, Brazil
gabriel.caldeira@lva.ufsc.br, mateus.grassano@polo.ufsc.br, julio.cordioli@ufsc.br, deschamps@polo.ufsc.br

Abstract. *The use of VLES-based Lattice Boltzmann methods in Computational Aeroacoustics (CAA) has gained attention due to their lower computational time compared to classical LES. However, these methods face challenges in accurately predicting the transition from laminar to turbulent flow. To address this, a zigzag-shaped protuberant structure is added to the propeller walls to disturb the boundary layer and transition from modeled turbulence to scaled turbulence calculations. In this study, a numerical investigation using VLES Lattice Boltzmann is conducted on a three-bladed NACA 5868-9 propeller to analyze the aerodynamic and acoustic effects of the zigzag tripping at different chord positions along the propeller radius. The tripping position was predicted using a low-order aerodynamic method based on the panel technique. The CAD model of the propeller was simulated in PowerFLOW, which uses the VLES Lattice Boltzmann method. The predictions without the zigzag tripping were validated and showed agreement with experimental data. With the inclusion of zigzag tripping, thrust and torque differed by approximately 10-20%, indicating its potential to alter the boundary layer and influence propeller loads. The study aims to provide preliminary insights into fluid mechanisms, spectral analysis of propeller noise emissions, and assess the advantages and disadvantages of the zigzag tripping strategy for improving CAA accuracy.*

Keywords: *Lattice-Boltzmann method, Zigzag tripping, NACA 5868-9 propeller, Aerodynamics, Aeroacoustics.*

1. INTRODUCTION

The rapid growth of distributed electric propulsion systems, such as electric Vertical Take-Off and Landing (eVTOL) vehicles, due to urban mobility demands Rajendran and Sharan (2020) and climate changing pressure Ren and Leslie (2019) requires careful consideration of design features. Considering its well-known reduced range due to batteries energy limitations Rohacs and Rohacs (2019), energy efficiency and high propulsive efficiency, and low noise emission to ensure acceptability in urban environments are desirable. The latter feature, i.e, low noise emission, is one of the most critical, considering their proximity to urban areas. To adhere to community noise standards (ICAO (2008)), predicting aircraft noise emissions is crucial and challenging, as low flying speeds over urban centres imply that the primary noise sources will be from the rotors or propellers, rather than the aircraft structure.

Propeller noise can be classified into two main spectral components: tonal and broadband noise. The former arises periodically, primarily from deterministic sources such as propeller aerodynamic loads. In contrast, the latter is generated by turbulence and vortex effects Kurtz and Marte (1970) and is the most challenging to predict. Recently, the use of the Very Large Eddy Simulation (VLES) Lattice-Boltzmann method, implemented in PowerFLOW Yakhot and Orszag (1986); Yakhot *et al.* (1992); Chen *et al.* (2003, 2004); Shan *et al.* (2006); Zhang *et al.* (2006); Chen *et al.* (2008, 2020), has gained attention. This is given its ability to predict propeller noise with an accuracy margin of 1 to 5 dB compared to experiments while requiring only a quarter of the computational effort needed for classical Large Eddy Simulations Gonzalez-Martino *et al.* (2018).

Although the VLES Lattice-Boltzmann method is promising, challenges arise in the case of low-Mach number propellers, $M < 0.5$, as classified by Jeracki and Mitchell (1981). In their work with PowerFLOW, Casalino *et al.* (2021) encountered difficulties in initiating the turbulent boundary layer transition for a 300mm diameter, dual-bladed propeller. To overcome this, they introduced a protuberant zigzag structure (less than 0.2mm in height) on the propeller wall, forcing the VLES solver to transition from modeled to scaled turbulence. The location of this structure was determined using a 2D panel method, prior to the main VLES simulation, relying on XFOIL Drela and Giles (1987). Although this work focuses on the computational aspect of zigzag tripping, the usage of the zigzag tripping is a well-known strategy in experiments, particularly with wind turbines, to force a fully developed turbulent boundary layer Alber *et al.* (2020); Gomez-Iradi and Munduate (2014); Alber *et al.* (2019). Yet, questions about potential spurious noise contributions from this structure

persist. This led to the study by Romani *et al.* (2022a), which examined the same propeller described by Casalino *et al.* (2021). They found that the noise levels of the propeller were influenced by the height of the tripping, with noticeable superficial aerodynamic variations in the propeller's suction and pressure surfaces in respect to pressure and velocity magnitudes. However, when it came to the overall aerodynamic metrics of thrust and torque, no differences were noted. It is argued that various tripping configurations might produce diverse effects on the propeller's suction and pressure side, but, still, these effects ultimately compensate each other, leading to similar values for thrust and torque.

Numerous knowledge gaps exist regarding the inclusion of zigzag tripping as a strategy to enhance numerical VLES's predictive accuracy for propeller Computational Aeroacoustics (CAA). Given this context, the primary objective of this research is a focused numerical investigation of the aerodynamic and acoustic consequences of introducing a protuberant zigzag tripping on the surface of a propeller in computational domains. For that, a three-bladed propeller with a diameter of 3 meters, operating at 1000 RPM under varying freestream conditions is simulated in a Lattice-Boltzmann VLES numerical framework. This specific rotational speed was selected to ensure a propeller blade tip Mach number below 0.5, positioning it within the domain of low-Mach propellers, where the VLES method necessitates such resort for an adequate modeling of turbulence. This article is organized as follows: Section 2 discusses the computational methodology, including the software used, the geometry of the propeller, and the computational setup, including the computational domain. In Section 3, the results and discussion are presented, covering the aerodynamic performance, noise emissions, and an investigation of fluid characteristics. Section 4 provides conclusions and outlines potential future work. Section 5 includes acknowledgments. Section 6 presents the references, and finally, Section 7 concludes with a note of responsibility.

2. COMPUTATIONAL METHOD

2.1 Flow solver

The CFD software SIMULIA PowerFLOW version 2019-R4 from Dassault Systemes is used to calculate the fluid flow throughout the propeller and to perform aerodynamic and aeroacoustic simulations. PowerFlow utilizes the lattice Boltzmann method (LBM) with a wall-modeled Very Large Eddy Simulation (VLES) approach for turbulence modeling (Romani *et al.* (2022a)). The LBM discretizes the domain of the fluid and solves the Boltzmann equation by computing a density probability function $f(\mathbf{x}, t, \mathbf{v})$. In a nutshell, the method involves finding a particle at a position $\mathbf{x}$ at a time t and with a velocity $\mathbf{v}$. Here, $f(\mathbf{x}, t, \mathbf{v})$ is described in time via an effective collision operator modeled by Bhatnagar-Gross-Krook (BKG) (Romani *et al.* (2022a); Zweck *et al.* (2002)).

The LBM is employed on a Cartesian grid consisting of cubic volumetric elements called Voxels. These elements intersect the wall geometry using planar surface elements referred to as Surfels, thus this approach discretizes the surface into solid bodies. Using a discrete integration of the discrete distribution function, hydrodynamic quantities of interest like density and velocity can be determined. In contrast, ideal gas thermodynamics is utilized to determine all other physical quantities. For accounting the mesh movement in order to modelling the propeller's rotation physics, the computational domain is divided into two distinct frames: an outer-fixed reference frame and an inner Local Reference Frame (LRF), the latter fixed to the body. The LRF is characterized by a mesh region that rotates in synchrony with the rotating geometry. In order to connect the two fluid flow regions, a mesh interface is utilized between the rotating and non-rotating inertial frames.

To mitigate the computational cost associated with accurately resolving acoustic wave propagation in the far-field, a far-field acoustic analogy is employed in this study. The computation of the far-field, kinematics and pressure distributions from the body geometry are computed using the impermeable Fflowcs-Williams and Hawkings' (FW-H) acoustic analogy. The FW-H solver utilized is part of the post-processing software SIMULIA PowerACOUSTICS and it is numerically implemented by means of a forward-time solution of Farassat's formulation 1A Farassat (2007). In acoustics, the acoustic field can be studied in terms of monopole, dipole, or quadrupole sources. Each of these source types is associated with the scattering of sound and the nature of the emitted sound waves. The formulation mentioned in this paper considers only distributions of acoustic monopoles and dipoles, commonly referred to as 'thickness' and 'loading' terms when describing the propeller's surface, respectively. However, it is important to note that this formulation does not take into consideration the contribution of quadrupole sources. This last source term can be neglected for propellers operating at low blade tip Mach number, as its wake is expected to produce negligible quadruple acoustic sources, as dipole noise sources are more efficient than the quadrupoles in this scenario (Romani *et al.* (2022a)).

2.2 Propeller geometry and computational setup

To accurately simulate the NACA 5868-9 three-bladed propeller illustrated in Figure 1, the 3D digital geometry or CAD (Computer Aided Design) was reconstructed based on the geometry provided in Biermann and Hartman (1939). The initial step involved extracting the pertinent details from the report, including the airfoil profile in its cross section, the distribution of the chord, sectional pitch angle (or twist), and thickness. The geometric distributions obtained from the report were then interpolated using a tenth-degree polynomial, as illustrated in Figure 1c. The relative chord with respect

to the propeller radius, pitch in degrees, and thickness relative to the chord were plotted with respect to their respective positions along the blade span.

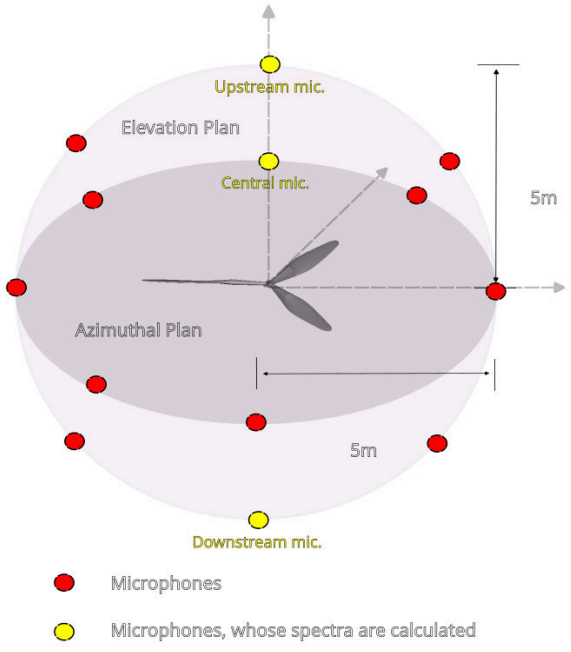

(a) Propeller rendered

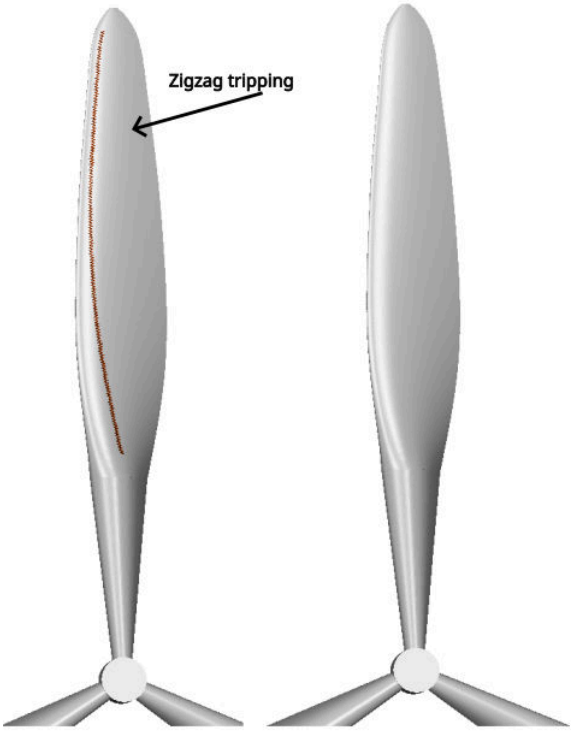

(b) Propeller rendered

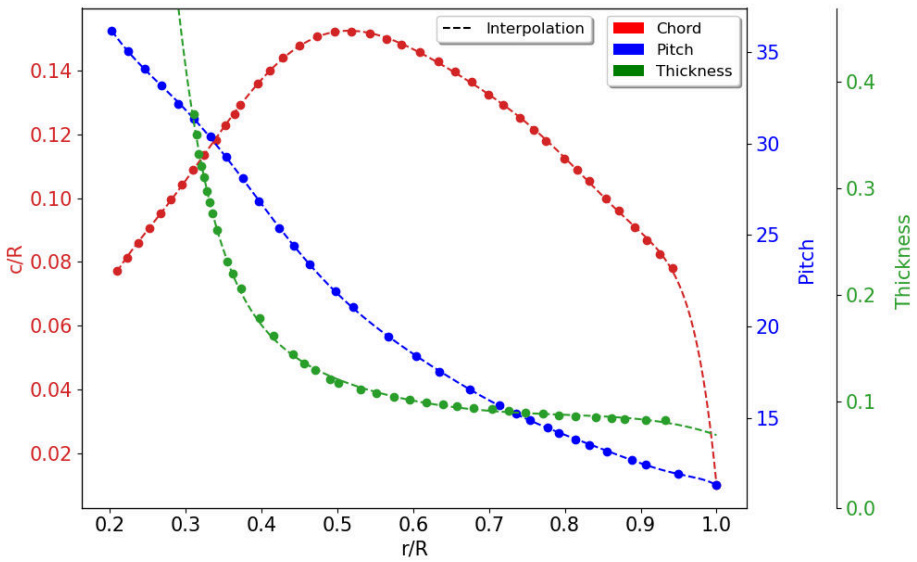

(c) Geometric distribution for the propeller's chord relative to the propeller radius, thickness, and section pitch angle.

Figure 1: Propeller geometry

Finally, the obtained geometric distribution can be easily imported into OpenSCAD, a scriptable 3D CAD generator OpenSCAD (2021) that operates on an open-source platform. Notably, Figure 1a visually represents the definitive geometry, encompassing the hub and the three blades, thereby showcasing the complete propeller structure. It is imperative to import this particular geometry into the simulations to ensure accurate and comprehensive analysis.

The far-field propagation is based on the microphone positions depicted in Figure 1a. In this figure, the configuration of 13 microphones employed in the study is shown. Six microphones are positioned in the azimuthal plane of the propeller, while the remaining seven are arranged perpendicularly to it in its elevation plane. A uniform distribution is achieved by

placing the microphones on a circle with a 5-meter radius. The calculated pressure time signals for these microphones are processed in terms of noise levels using two frequency domain metrics, Overall Acoustics Sound Pressure Level (OASPL) for frequency bands between a half of its Blade Passing Frequency (BPF) and 10kHz, and narrow band spectra. The OASPL for all microphones is calculated to obtain the directivity in both the azimuthal and elevation planes of the propeller. The narrow band spectra are obtained only for the upstream, central and downstream microphones, illustrated in yellow. These results, obtained in spectral density units, are analyzed using Welch's method, as described by Shin and Hammond (2008). Such analysis aims to study the noise levels across different frequency bands, with particular attention to tonal and broadband components.

The propeller under investigation is subjected to a constant angular velocity of 1000 RPM. The study explores advance ratios ranging from $J = 0.1$ to 0.8. The advance ratio is defined as the ratio of the free-stream velocity V_∞ to the product of the propeller's revolutions per second n and diameter D ($J = V_\infty/(nD)$). The free-stream velocity is varied from 0 to 40 m/s across this range of advance ratios. It is important to note that V_∞ is directed parallel to the propeller axis. By manipulating the free-stream velocity, the propeller's performance and noise characteristics can be comprehensively assessed at different operating conditions, providing valuable insights into its behavior and enabling a thorough analysis of the trailing edge noise.

In the computational setup, the fluid domain was defined as a spherical volume with a radius of 650m, strategically centered around the propeller's center. To ensure accurate simulations and replicate an anechoic environment, an acoustic sponge was placed in the edges of this volume, this was numerical modelled as a region where a progressively increment of the turbulent viscosity is defined. This acoustic sponge served the purpose of effectively dissipating sound waves and preventing their reflection within the computational domain. Specifically, the acoustic sponge was implemented as an arrangement of two concentric spheres with distinct radius of 122m and 480m, respectively. Both spheres were carefully centered around the propeller, ensuring the definition of a acoustic sponge absorbing region. By incorporating this advanced acoustic sponge technique, the computational setup successfully recreated a controlled anechoic environment for accurate analysis and interpretation of the acoustic phenomena surrounding the propeller.

The zig-zag transition trip was employed on the suction side of the blade as a numerical approach, firstly promoting the formation of vortical structures, and finally enabling the turbulence to transition from a modeled state to a scale-resolved state. Therefore, in theory, embedding the method's predictive capacities. The zig-zag topology is preferred due to its high efficiency and low critical roughness, which initiates transition even at low Reynolds numbers. A designated trip height of 2.4 mm, equivalent to 3 voxels (the term for discretized cells in PowerFLOW), ensures accurate discretization near the tripping region, given the computational mesh in use. On the other hand, no trip is introduced on the pressure side of the propeller, as the laminar to turbulent boundary layer transition is expected to occur spontaneously, as predicted by the BEMT/viscous panel method code Drela and Giles (1987).

For the mesh parameters, voxel refinement ranges from 0.80 mm to 5.3 m. Additional details about this mesh, when applied to propellers, can be found in Lattari *et al.* (2023). The simulations account for 10 rotations for domain initialization and take measurements from four subsequent rotations, resulting in a overall 600k time steps, equating to a physical duration of 0.720 seconds.

Lastly, the experimental measurements, which are meant for simulation validation, are sourced from Biermann and Hartman (1939). The propeller testing methodology in the wind tunnel consisted of keeping the propeller speed unchanged and incrementing the tunnel speed in stages until reaching a peak of 115 miles per hour (51.41 m/s). The selection of this particular propeller was based on its well-documented results and geometry, especially given the age of the data. This rationale has also been adopted in other contemporary studies Venusamy *et al.* (2023); Cong *et al.* (2023).

3. RESULTS AND DISCUSSION

3.1 Aerodynamic Performance

In order to compute the thrust (C_T) and power (C_P) coefficients, and propulsive efficiency (η) at different advance ratios, the following equations were used, namely

$$C_T = \frac{T}{\rho n^2 D^4}, \quad (1) \qquad C_P = \frac{P}{\rho n^3 D^5}, \quad (2) \qquad \eta = \frac{J C_T}{C_P}. \quad (3)$$

, where: T: is the Thrust force, ρ is the air density of the fluid, n: Rotational speed (revolutions per second), D is the Diameter of the propeller, P is the power input and J is the advance ratio.

Comparisons between numerical results and experimental measurements from Biermann and Hartman (1939) (Figure 2a), which include numerical results both with and without the inclusion of the zigzag tripping, demonstrate agreement for the coefficients of thrust and torque up to J=0.6, with a maximum deviation of 12.9% in the value of C_t when compared to experimental results, observed exclusively for the non tripped case. The tripping inclusion exhibits deviations from

measurements close to 40%. The results incorporating the tripping were computed only for J=0.2 and 0.6, leading to a substantial impact on aerodynamic efficiency. Beyond J=0.6 point, however, the torque is significantly overestimated, even for the prediction without the tripping, resulting in a discrepancy in aerodynamic efficiency of up to 50%.

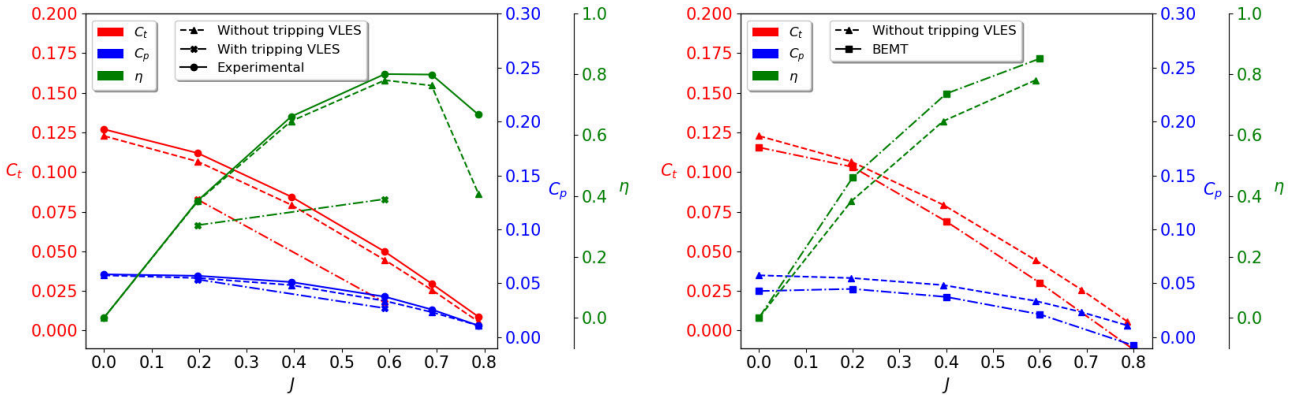

(a) Numerical vs. experimental results with and without tripping

(b) VLES without tripping versus BEMT.

Figure 2: Validation for PowerFLOW (with and without tripping) and BEMT model - tripping position calculated automatically

Given that the positioning of the tripping in the numerical simulations is based on the expected turbulent transition location of the boundary layer, as computed by the 2D panel method, it is essential to validate its results against the VLES simulation implementing it to a Blade Element Momentum Theory (BEMT) model that does not incorporate the structure. According to Figure 2b, findings reveal that the deviation tends to increase as the advance ratio (J) becomes larger, exhibiting significant deviation (over 50%) for J values exceeding 0.6. Consequently, the investigation into tripping is confined to this maximum J value.

3.2 Noise Emissions

The subsequent analysis is carried out for the J=0.2 case, as it is representative of the phenomena under investigation and similar results are obtained from other advance ratios. The time-varying pressure signal and the corresponding spectra for the upstream microphone are illustrated in Figure 3. The results suggest that the inclusion of tripping results in less pressure fluctuations, as further validated by the spectra. In this case, the broadband noise at frequencies above 1kHz displays lower values for the case with tripping. This finding is corroborated for the central microphone (Figure 4), although the fluctuations are less pronounced in this instance. The downstream microphone, depicted in Figure 5, present a similar situation, although the fluctuations are marginally more intense than those observed for the central microphone. The outcomes of this analysis strongly suggest that the introduction of tripping may be expediting the transition of the boundary layer to a turbulent state. This is due to the fact that laminar instability is likely to generate more noise in moderate broadband frequency bands (1kHz to 10kHz) Grande *et al.* (2022).

Examining the azimuthal plane directivity, as illustrated in Figure 6a, results indicate that the data without tripping presents higher levels of OASPL for all microphone directions compared to the tripping counterparts. This reveals a less complex pattern. When observing the elevation plane directivity, portrayed in Figure 6b, the non-inclusion of tripping displays a well-defined dipole pattern, similar to those observed in Romani *et al.* (2022b). However, for the microphones levels with the inclusion of the tripping, no dipole pattern is obtained, highlighting an indicative of less physical background of the zigzag tripping.

3.3 Fluid characteristics investigation

The coefficient of pressure (C_p), which is a dimensionless quantity that represents the pressure relative to the total pressure on a surface, and the vorticity magnitude (Anderson (2010)) are selected as primary metrics in this noise sources investigation, as these variables can represent blade loading and fluid behaviour respectively. Those are both critical contributors to broadband noise, as suggested by Kurtz and Marte (1970). The C_p contours on the propeller's suction surface, where the zigzag tripping is initially placed, is depicted in Figure 7. Moreover, the fluid streamlines are also captured to provide an in-depth understanding of the flow dynamics. The findings suggest that the introduction of tripping leads to higher pressure values in its immediate vicinity, this is likely to be a cause of the reduced thrust result generated by the tripping inclusion. The vorticity magnitude at the propeller's trailing-edge further illustrates that the inclusion of this structure has the potential to alleviate some of its intensity and also can be related to the low values of noise in high frequencies depicted in Figures 3, 4 and 5. This observation is further corroborated by a more focused examination of the

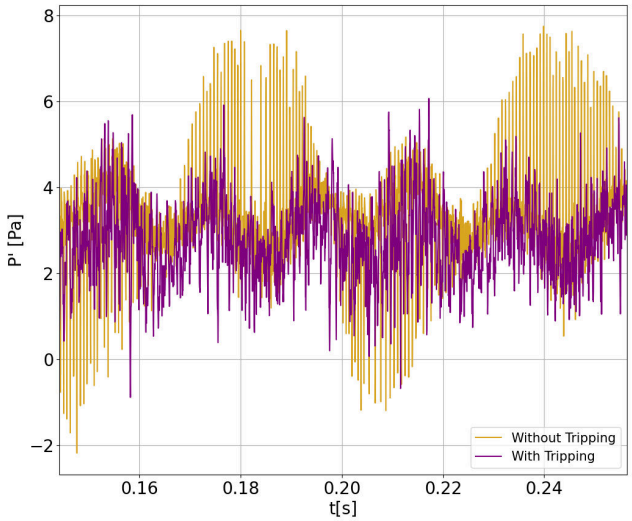

(a) Pressure Signal for the upstream microphone

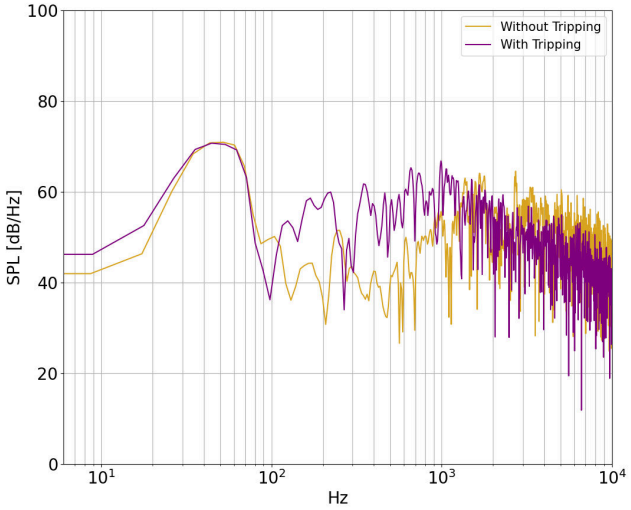

(b) Spectrum for the upstream microphone

Figure 3: Acoustic data for the upstream microphone

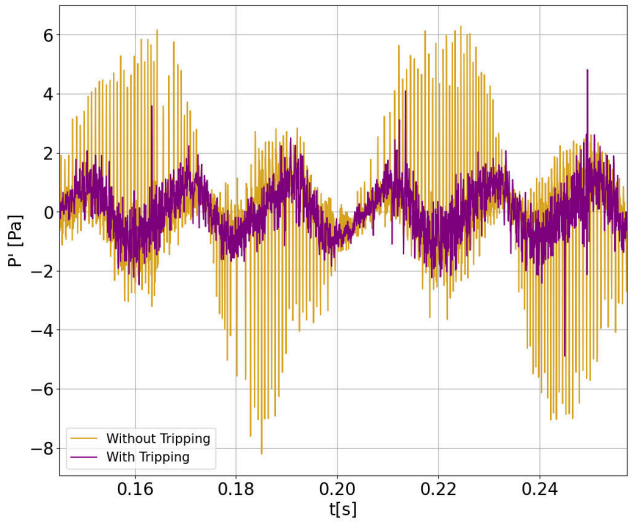

(a) Pressure Signal for the central microphone

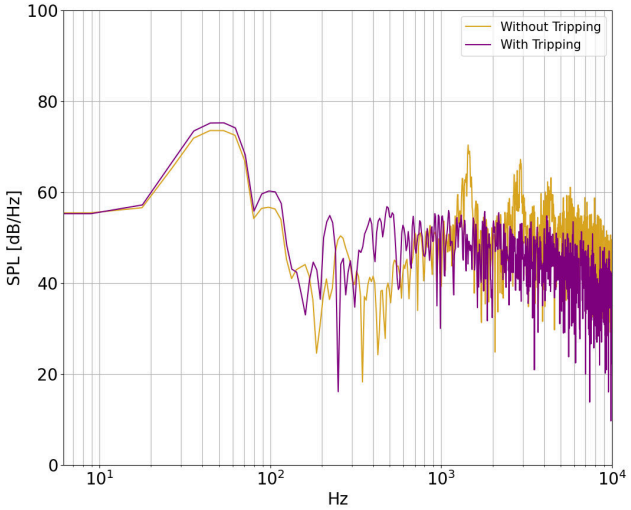

(b) Spectrum for the central microphone

Figure 4: Acoustic data for the central microphone

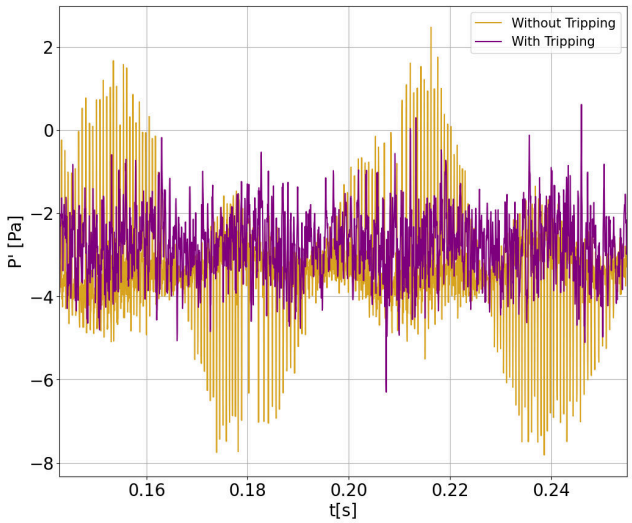

(a) Pressure Signal for the downstream microphone

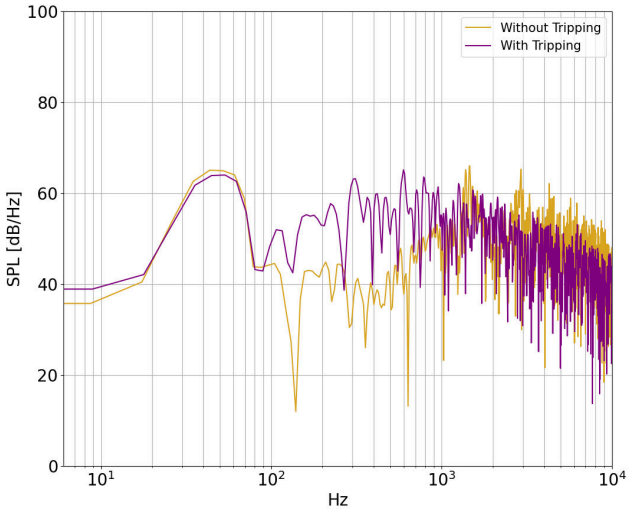

(b) Spectrum for the downstream microphone

Figure 5: Acoustic data for the downstream microphone

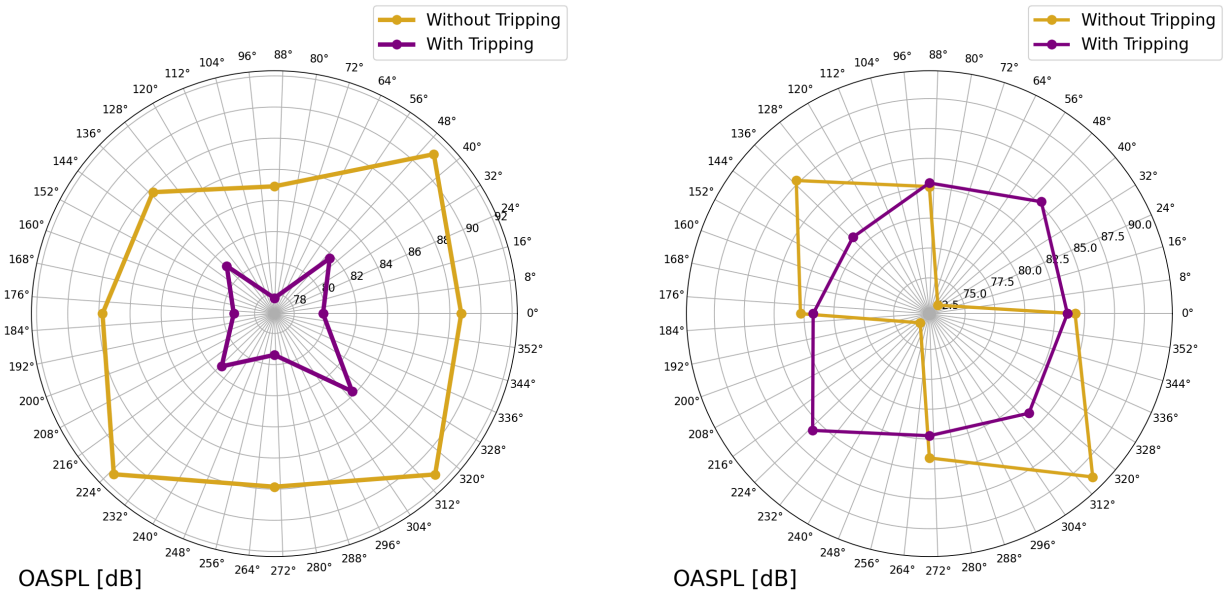

(a) Directivity for the azimuthal plan (b) Directivity for the elevation plan

Figure 6: Directivity for azimuthal and elevation plans

propeller's surface, as illustrated in Figure 8. The streamlines clearly demonstrate how the incorporation of the tripping structure in the simulation can cause deformation and disrupt the fluid flow patterns. This could possibly indicate a forced transition of the boundary layer to a turbulent state.

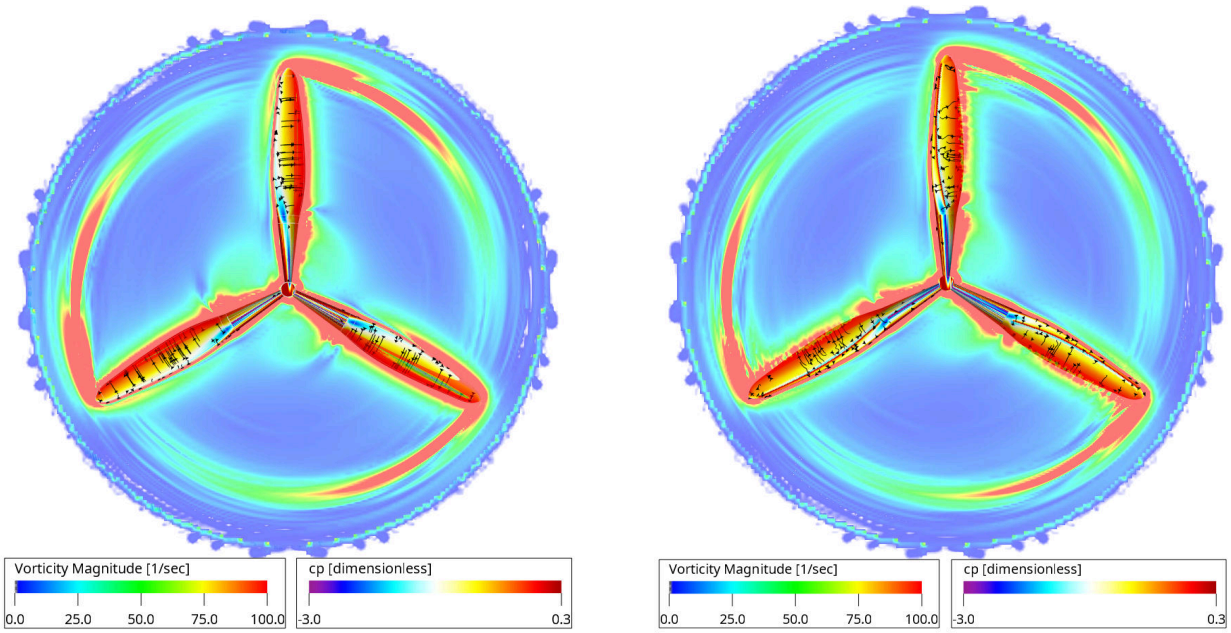

(a) Without tripping (b) With tripping

Figure 7: Cp contour for the propeller and vortex magnitude contours in the propeller's azimuthal plane (suction surface)

In this investigation, a particular focus is driven towards the analysis of vorticity magnitude contours, with a specific focus on cross-sections at various radial positions. Given the tri-blade configuration, a preliminary assessment indicates that all three blades exhibit analogous results. The outcomes for a representative section at r/R=0.75 for one blade are illustrated in Figure 9. This figure contrasts predictions both with and without tripping. Notably, the findings suggest that the vorticity magnitude in the trailing-edge wake is more pronounced for the case without tripping than for the case with it. Additionally, Figure 9 highlights the voxels forming the mesh used in the computational setup for the fluid domain. However, employing a more sophisticated technique, such as correlation analysis, might offer further insights and validation for this observation.

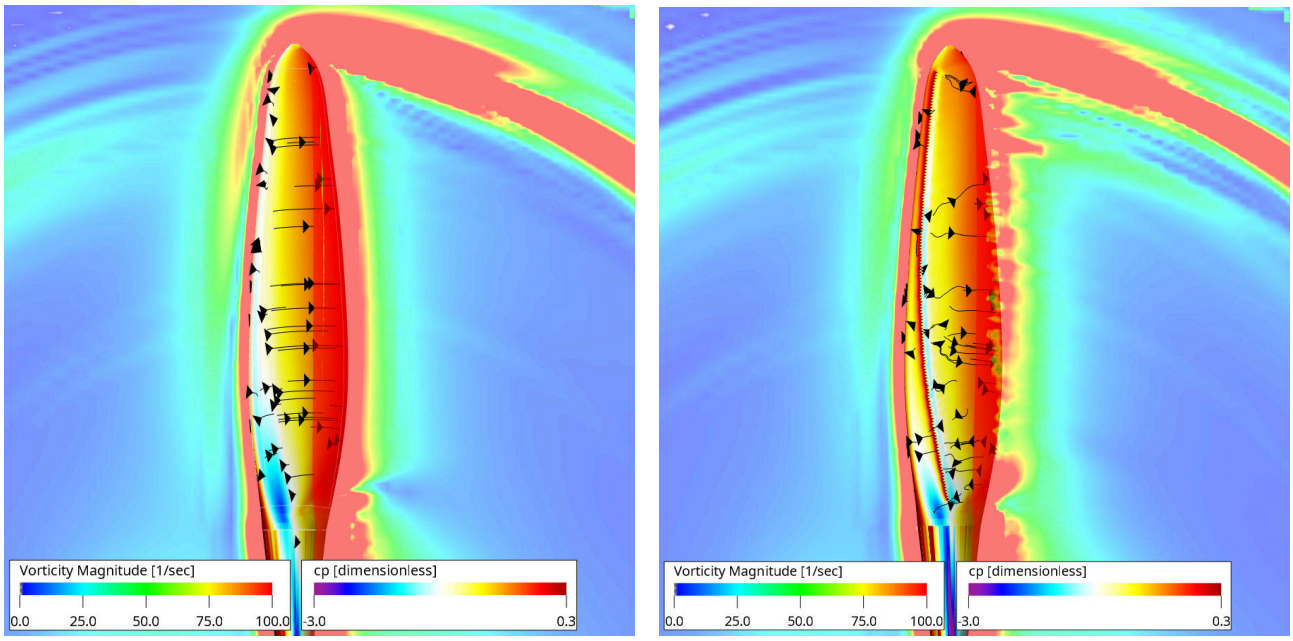

(a) Without tripping (b) With tripping

Figure 8: Closer details of the Cp contour for the propeller and vortex magnitude contours in the propeller's azimuthal plane (suction surface)

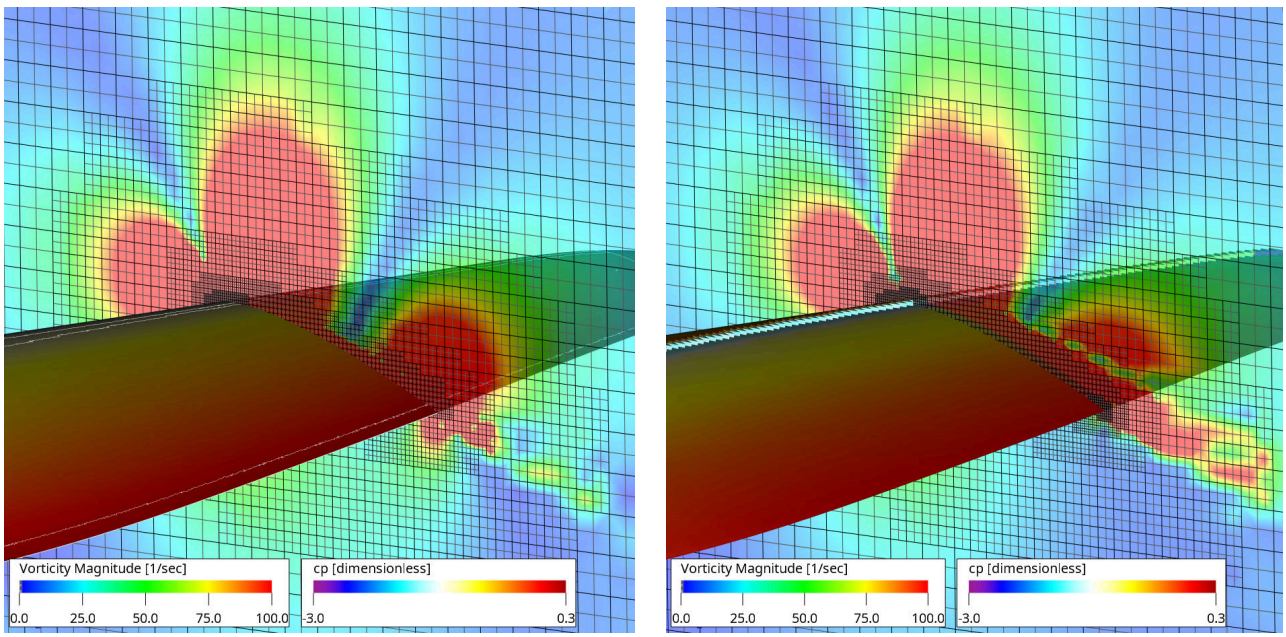

(a) Without tripping (b) With tripping

Figure 9: Closer details of the mesh employed to compute fluid data for a representative section at $r/R = 0.75$

4. CONCLUSIONS

The growing interest for electric aviation and the upcoming usage of propellers powered aircraft in the vicinities of urban areas raises serious questions about noise. Still, much knowledge gaps exist in the numerical simulations using Lattice Boltzmann VLES in PowerFLOW, especially surrounding the zigzag tripping inclusion for triggering the propeller's boundary layer transition to turbulence for embedding VLES numerical predictive capabilities. In these preliminary results, it was shown that the tripping inclusion disrupts the aerodynamic behaviour of the propeller in respect to experimental results, resulting in deviation close to 40% for thrust and torque, it was also observed lower broadband noise levels by its inclusion, up to 1kHz frequency bands and a lost of coherence of the dipole pattern for propeller OASPL directivity. The fluid flow analysis of the pressure coefficient and vorticity magnitude confirmed this tendency, as the tripping inclusion increased the pressure in the blade's suction side as well as diminishing the vortex magnitude beyond its trailing edge.

Some question still remains, considering the great impact of the tripping in the aerodynamic performance of this propeller. In future work, it is expected that more tripping configurations are ought to be tested, especially by varying its height and position or further improving the positioning algorithm.

5. ACKNOWLEDGEMENTS

The authors appreciate the support from EMBRAER and EMBRAPII, as well as the additional funding provided by the National Institutes of Science and Technology (INCT) Program.

6. REFERENCES

Alber, J., Nayeri, C., Paschereit, C., Twele, J. and Fortmann, J., 2019. "Mini-gurney flaps for aerodynamic optimizations of hawt rotor blades".

Alber, J., Soto-Valle, R., Manolesos, M., Bartholomay, S., Nayeri, C.N., Schönlau, M., Menzel, C., Paschereit, C.O., Twele, J. and Fortmann, J., 2020. "Aerodynamic effects of gurney flaps on the rotor blades of a research wind turbine". *Wind Energy Science*, Vol. 5, No. 4, p. 1645–1662. doi:10.5194/wes-5-1645-2020. URL https://wes.copernicus.org/articles/5/1645/2020/.

Anderson, J., 2010. *Fundamentals of Aerodynamics*, McGraw-Hill Education. ISBN 9780073398105. URL https://books.google.com.br/books?id=xwY8PgAACAAJ.

Biermann, D. and Hartman, E.P., 1939. "The aerodynamic characteristics of six full-scale propellers having different airfoil sections".

Casalino, D., Grande, E., Romani, G., Ragni, D. and Avallone, F., 2021. "Definition of a benchmark for low reynolds number propeller aeroacoustics". *Aerospace Science and Technology*, Vol. 113, p. 106707. ISSN 1270-9638. doi:https://doi.org/10.1016/j.ast.2021.106707. URL https://www.sciencedirect.com/science/article/pii/S1270963821002170.

Chen, H., Goldhirsch, I. and Orszag, S., 2008. "Discrete rotational symmetry, moment isotropy, and higher order lattice boltzmann models". *J. Sci. Comput.*, Vol. 34, No. 1, pp. 87–112. doi:10.1007/s10915-007-9159-3. URL https://doi.org/10.1007/s10915-007-9159-3.

Chen, H., Kandasamy, S., Orszag, S., Succi, S. and Yakhot, V., 2003. "Extended boltzmann kinetic equation for turbulent flows". *Science*, Vol. 301, No. 5633, pp. 633–636. doi:10.1126/science.1085048. URL https://doi.org/10.1126/science.1085048.

Chen, H., Orszag, S., Staroselsky, I. and Succi, S., 2004. "Expanded analogy between boltzmann kinetic theory of fluid and turbulence". *J. Fluid Mech.*, Vol. 519, pp. 301–314. doi:10.1017/S0022112004001211. URL https://doi.org/10.1017/S0022112004001211.

Chen, H., Zhang, R. and Gopalakrishnan, P., 2020. "Filtered lattice boltzmann collision formulation enforcing isotropy and galilean invariance". *Phys. Scr.*, Vol. 95, No. 3, p. 034003. URL https://doi.org/10.1088/1402-4896/ab7737.

Cong, K., Ma, D., Zhang, L., Xia, X. and Yao, Y., 2023. "Design and analysis of passive variable-pitch propeller for vtol uavs". *Aerospace Science and Technology*, Vol. 132, p. 108063. ISSN 1270-9638. doi:10.1016/j.ast.2022.108063. URL https://www.sciencedirect.com/science/article/pii/S1270963822007374.

Drela, M. and Giles, M., 1987. "Viscous-inviscid analysis of transonic and low reynolds number airfoils". *AIAA Journal*, Vol. 25, No. 10, pp. 1347–1355.

Farassat, F., 2007. "Derivation of formulations 1 and 1a of farassat". Technical report.

Gomez-Iradi, S. and Munduate, X., 2014. "Zig-zag tape influence in nrel phase vi wind turbine". *Journal of Physics: Conference Series*, Vol. 524, p. 012096. doi:10.1088/1742-6596/524/1/012096.

Gonzalez-Martino, I., Romani, G., Wang, J. and Casalino, D., 2018. "Rotor noise generation in a turbulent wake using lattice-boltzmann methods". In *2018 AIAA/CEAS Aeroacoustics Conference*. p. 3447.

Grande, E., Romani, G., Ragni, D., Avallone, F. and Casalino, D., 2022. "Aeroacoustic investigation of a propeller operating at low reynolds numbers". *AIAA Journal*, Vol. 60, No. 2, pp. 860–871. doi:10.2514/1.J060611. URL https://doi.org/10.2514/1.J060611.

ICAO, 2008. "ANNEX 16". 5th edition, incorporating Amendments 1-9.

Jeracki, R. and Mitchell, G., 1981. "Low and high speed propellers for general aviation – performance potential and recent wind tunnel test results". In *SAE Technical Paper*. 811090. URL https://doi.org/10.4271/811090.

Kurtz, D.W. and Marte, J.E., 1970. "A review of aerodynamic noise from propellers, rotors, and lift fans".

Lattari, M.G., Rosa, V.H. and Deschamps, C.J., 2023. *Numerical Analysis of Aerodynamics and Acoustics of a Variable Pitch Propeller*. doi:10.2514/6.2023-4053. URL https://arc.aiaa.org/doi/abs/10.2514/6.2023-4053.

OpenSCAD, 2021. "Openscad - the programmers solid 3d cad modeller". URL https://www.openscad.org/. Version 2021.01.

Rajendran, S. and Sharan, S., 2020. "Air taxi service for urban mobility: A critical review of recent developments, future challenges, and opportunities". *Transportation Research Part E: Logistics and Transportation Review*, Vol. 143, p. 102090. ISSN 1366-5545. doi:10.1016/j.tre.2020.102090. URL https://www.sciencedirect.com/science/article/pii/S1366554520307390.

Ren, D. and Leslie, L.M., 2019. "Climate warming and effects on aviation". In R.K. Agarwal, ed., *Environmental Impact of Aviation and Sustainable Solutions*, IntechOpen, Rijeka, chapter 9. doi:10.5772/intechopen.86871. URL https://doi.org/10.5772/intechopen.86871.

Rohacs, J. and Rohacs, D., 2019. "Conceptual design method adapted to electric/hybrid aircraft developments". *International Journal of Sustainable Aviation*, Vol. 5, No. 3.

Romani, G., Grande, E., Avallone, F., Ragni, D. and Casalino, D., 2022a. "Performance and noise prediction of low-reynolds number propellers using the lattice-boltzmann method". *Aerospace Science and Technology*, Vol. 125. ISSN 12709638. doi:10.1016/j.ast.2021.107086.

Romani, G., Grande, E., Avallone, F., Ragni, D. and Casalino, D., 2022b. "Computational study of flow incidence effects on the aeroacoustics of low blade-tip mach number propellers". *Aerospace Science and Technology*, Vol. 120. ISSN 12709638. doi:10.1016/j.ast.2021.107275.

Shan, X., Yuan, X.F. and Chen, H., 2006. "Kinetic theory representation of hydrodynamics: a way beyond the navier-stokes equation". *J. Fluid Mech.*, Vol. 550, p. 413. doi:10.1017/S0022112005008153. URL https://doi.org/10.1017/S0022112005008153.

Shin, K. and Hammond, J., 2008. *Fundamentals of Signal Processing for Sound and Vibration Engineers*. Wiley. ISBN 9780470725641. URL https://books.google.com.br/books?id=Lukr9uCCQKYC.

Venusamy, K., R, S.N., Sam, D. and John, B.W., 2023. "Study and outline of vertical take-off and landing (vtol) system". In *2023 Second International Conference on Electronics and Renewable Systems (ICEARS)*. pp. 108–114. doi:10.1109/ICEARS56392.2023.10085366.

Yakhot, V. and Orszag, S., 1986. "Renormalization group analysis of turbulence. i. basic theory". *J. Sci. Comput.*, Vol. 1, No. 1, pp. 3–51. doi:10.1007/BF01061452. URL https://doi.org/10.1007/BF01061452.

Yakhot, V., Orszag, S., Thangam, S., Gatski, T. and Speziale, C., 1992. "Development of turbulence models for shear flows by a double expansion technique". *Phys. Fluids A*, Vol. 4, No. 7, pp. 1510–1520. doi:10.1063/1.858424. URL https://doi.org/10.1063/1.858424.

Zhang, R., Shan, X. and Chen, H., 2006. "Efficient kinetic method for fluid simulation beyond the navier-stokes equation". *Phys. Rev. E*, Vol. 74, No. 4, p. 046703. doi:10.1103/PhysRevE.74.046703. URL https://doi.org/10.1103/PhysRevE.74.046703.

Zweck, C., Freymueller, J.T. and Cohen, S.C., 2002. "Extended boltzmann kineticequation for turbulent flows". *Journal of Geophysical Research: Solid Earth*, Vol. 107. ISSN 21699356. doi:10.1029/2001jb000409.

7. RESPONSIBILITY NOTICE

The authors, Gabriel Caldeira Vicente, Mateus Grassano Lattari, Júlio Apolinário Cordioli, and César José Deschamps, are solely responsible for the printed material included in this paper.